

Quantum-chromodynamic gluon contributions to large- p_T reactions*

Roger Cutler and Dennis Sivers

High Energy Physics Division, Argonne National Laboratory, Argonne, Illinois 60439

(Received 11 July 1977)

We use a calculation based on the lowest order in the perturbation series for quantum chromodynamics to obtain an estimate for the contribution of hard-scattering processes involving vector gluons to the production of hadrons at large transverse momentum. Some simple models for the distribution of gluons in a proton and for the distribution of hadrons within a hard gluon jet are presented and used to calculate the process $pp \rightarrow \pi^0 X$. At $\sqrt{s} = 53$ GeV we find that the contribution of the subprocess $qV \rightarrow qV$ is comparable to that of $qq \rightarrow qq$. The resulting cross sections are rather close to the CERN ISR data in magnitude. It is possible that small corrections arising, for example, from higher-order terms in the perturbation expansion might lead to a detailed fit to these data. At higher energies, such as those to be obtained in proposed new experimental facilities, our results indicate that the mechanisms $VV \rightarrow VV$ and $qV \rightarrow qV$ may dominate over $qq \rightarrow qq$ in much of the accessible kinematic regime. We briefly consider some experimental consequences of possible gluon dominance.

I. INTRODUCTION

Taking a liberal interpretation of the idea of asymptotic freedom, we may hope that the usual perturbation expansion can provide a guide to the behavior of quantum chromodynamics (QCD) at large momentum transfer. This speculation has some interesting implications for the production of hadrons at large p_T , since the large transverse momentum can arise from the hard interaction of elementary constituents. Starting with the original proposal of Berman, Bjorken, and Kogut,¹ many models have been constructed²⁻⁵ in which the dominant mechanism involves the scattering of quarks. For example, in a previous paper⁶ we discuss how the one-gluon-exchange approximation to $qq \rightarrow qq$ could be normalized, and we estimated its contribution to $pp \rightarrow \pi^0 X$ at large p_T . We found the contribution of this mechanism to be slightly below CERN ISR data at $\sqrt{s} = 53$ GeV, $p_T \geq 6$ GeV.

However, if QCD and perturbation theory are indeed to be a guide to large- p_T production, it is probably not sufficient to consider only a $qq \rightarrow qq$ scattering mechanism. In addition to quarks, hadrons are presumed to contain colored vector gluons which can scatter off quarks or other gluons in an approximately scale-invariant manner. The presence of gluons explains why, in Ref. 6, we were careful to interpret the contribution of $qq \rightarrow qq$ as a lower bound for the production of hadrons at very large p_T .

We would now like to be more thorough. We will therefore systematically examine all the fundamental QCD processes which can contribute an approximately scale-invariant piece,

to the invariant cross section. We calculate the cross sections for the subprocesses $qq \rightarrow qq$, $\bar{q}\bar{q} \rightarrow \bar{q}\bar{q}$, $q\bar{q} \rightarrow q\bar{q}$, $qV \rightarrow qV$, $\bar{q}V \rightarrow \bar{q}V$, $\bar{q}q \rightarrow VV$, $VV \rightarrow \bar{q}\bar{q}$, and $VV \rightarrow VV$ (where V stands for vector gluon) to lowest order in perturbation theory and use the results in the hard-scattering model for $pp \rightarrow \pi^0 X$. This procedure should be approximately correct at very large momentum transfer where the effective quark-gluon coupling constant is small.

In order to calculate the contribution of gluonic processes to the hard-scattering model for $pp \rightarrow \pi^0 X$, one must know the momentum distributions of gluons and quarks within the proton and the probability distribution for a scattered gluon or quark to produce a hadron. The necessary distributions for quarks can be measured in processes involving leptons. For gluons we must resort to indirect arguments and intuition based on simple theoretical models. Our results at ISR energies are somewhat sensitive to these distributions, and we therefore consider a range of possibilities.

Throughout this paper we will be calculating to lowest order in the QCD perturbation series. This means that we will be ignoring a host of higher-order correction terms which are not necessarily small. We thus expect to find only an approximate guide to the implications of QCD for high- p_T inclusive processes, and we do not expect, nor would we believe, detailed fits to data resulting from these lowest-order calculations. However, we will find that this approach will yield cross sections which are close enough to the ISR data so that one might *hope* that more detailed calculations will provide an overall agreement with high- p_T data.

The plan of this paper is as follows: In Sec. II we describe our estimates for the gluon distribu-

$$\frac{Ed^3\sigma}{d^3p} \sim \frac{f(p_T/\sqrt{s})}{p_T^4}, \quad (1.1)$$

tions. Section III considers the quark-gluon and gluon-gluon scattering cross sections, and discusses some technical complications of gluon spin sums and gauge invariance. In Sec. IV we present our calculations using the hard-scattering model for single-particle distributions. This section contains our main results. In Sec. V we discuss some implication for future experiments of gluon contributions to high- p_T production. For the convenience of the reader, we include two appendixes. The first contains the Feynman rules for QCD and the calculation of the cross sections we are considering. The second contains some identities for SU(3) matrices useful in doing color averaging.

II. GLUONS IN THE PROTON

We wish to calculate the contributions of processes involving gluons to the hard-scattering model for $pp \rightarrow \pi X$,³

$$\begin{aligned} \frac{E d^3\sigma}{d^3p} (pp \rightarrow \pi X) \\ \sim \frac{1}{\pi} \sum_{ab \rightarrow cd} \int dx_a dx_b G_{a/p}(x_a) G_{b/p}(x_b) \\ \times \frac{dz}{z^2} D_{\pi/c}(z) \left[\hat{s} \frac{d\sigma}{dt} (ab \rightarrow cd) \right] \\ \times \delta(\hat{s} + \hat{t} + \hat{u}), \end{aligned} \quad (2.1)$$

where the sum over partons (a, b, c, d) includes gluons as well as quarks. The model will now have ingredients which were not discussed in Ref. 6. The cross sections $d\sigma/dt$ for processes involving gluons will be presented in Sec. III and Appendix A. Here we will discuss how to estimate the probability, $G_{v/p}(x)$, of finding a vector gluon within a proton and the probability, $D_{\pi/v}(z)$, for a gluon to decay into a pion.

Unlike the situation for the process $qq \rightarrow qq$, where the analogous distributions are reasonably well known from measurements involving leptons, we have to rely on models to obtain gluon distributions. We believe that the current theoretical understanding of hadronic structure is not sufficient to determine these distributions in detail from first principles. So, following Aristotle's precept that "a well schooled man is one who searches for that degree of precision in each kind of study which the nature of the subject at hand admits," we will examine several different models for gluon distribution without worrying too much about theoretical rigor.

The starting point for this exercise must certainly be the momentum sum rule. In a parton model with exact scaling we can define the total fractional momentum carried by quarks and antiquarks in the proton to be

$$\langle x \rangle_{\text{charged}} = \int_0^1 dx x [u(x) + d(x) + s(x) + \bar{u}(x) + \bar{d}(x) + \bar{s}(x)] . \quad (2.2)$$

where $u(x) = G_{u/p}(x)$, and we neglect tiny contributions from heavier quarks (c, t, b, \dots). These quark distributions can be measured in deep-inelastic scattering, and in the Field-Feynman analysis³ of lepton data the terms in (2.2) are summed to give

$$\langle x \rangle_{\text{charged}} \cong 0.5 . \quad (2.3)$$

The remainder of the proton's momentum must be carried by neutral objects which do not couple to the electromagnetic or weak currents. If we identify these objects with vector gluons, we have the constraint

$$\int_0^1 x G_{v/p}(x) dx \cong 0.5 . \quad (2.4)$$

In principle, scale-violating effects such as those predicted⁷ by QCD will give the normalization condition (2.4) some logarithmic Q^2 dependence. However, these corrections are related to higher-order terms in the QCD perturbation series, and thus may be small if we confine our attention to kinematic regimes where the quark-gluon coupling constant, $\alpha_s(Q^2)$, is small. Since we are interested in getting a rough estimate of the relative size of gluon and quark contributions to large- p_T production, we will, in the remainder of this paper, neglect scaling violations in the distribution functions of both quarks and gluons. We can therefore use (2.4) to normalize our models for the gluon distribution function. We will keep an open mind on the subject of scaling violations, however, as they may be important in getting detailed fits to the data.⁵⁻⁷

The only problem remaining, therefore, is the shape of the gluon distribution. Our initial assumption is that the gluons are rapidly, perhaps exponentially, damped in transverse momentum. This approximately corresponds to having the gluons coexist with the quarks within hadrons of a finite size. We will not worry in any detail about the nature of the transverse momentum cutoff. The dependence on the x variable should, we believe, follow the general rule that the gluon distribution is softer than a valence-quark distribution and harder than a sea-antiquark distribution. Between these extremes there is a great deal of leeway, and we will demonstrate this by looking at specific models.

Naive model for $G_{v/p}(x)$

For the first model, we follow the analysis of Brodsky and Farrar⁸ and of Blankenbecler and

Brodsky⁹ and describe the behavior of the constituent distributions near $x=1$ in terms of the counting rules,

$$\lim_{x \rightarrow 1} G_{a/A}(x) = c(1-x)^{2n(\bar{a}A)-1}, \quad (2.5)$$

where $n(\bar{a}A)$ is the minimum number of elementary constituents left behind in the $\bar{a}A$ system. For quarks and gluons in the proton these assumptions give

$$\begin{aligned} G_{q/p}(x) &\sim c_q(1-x)^3, \\ G_{V/p}(x) &\sim c_V(1-x)^5, \\ G_{\bar{q}/p}(x) &\sim c_{\bar{q}}(1-x)^7. \end{aligned} \quad (2.6)$$

Near $x=0$, the behavior of distributions in the parton model is often presumed to be related to the Regge behavior of total cross sections.¹⁰ If $\sigma_{\bar{a}A} \propto s^{\alpha-1}$ then

$$\lim_{x \rightarrow 0} G_{a/A}(x) \sim \tilde{c}x^{-\alpha}. \quad (2.7)$$

Pomeron exchange, with $\alpha=1$, gives Feynman scaling for inclusive cross sections and we assume that

$$G_{V/p} \sim \frac{\tilde{c}_V}{x}. \quad (2.8)$$

In the absence of a more concrete model, we can assume that there is a smooth interpolation between (2.6) and (2.8) and write

$$G_{V/p}(x) \simeq \frac{3}{x}(1-x)^5, \quad (2.9)$$

where we have used (2.4) to fix the normalization. We compare this naive gluon distribution function with the Field-Feynman parametrization for $G_{u/p}(x)$ and $G_{\bar{u}/p}(x)$ in Fig. 1.

Bremsstrahlung model for $G_{V/p}(x)$

We can also make a slightly more complicated model for the gluon distribution by utilizing some of the concepts behind the constituent counting rules. Let us suppress all flavor and spin degrees of freedom and construct a simple picture of the proton which illustrates the relation between valence quarks, gluons, and the sea of quark-antiquark pairs.

In a zeroth-order picture a proton would consist of three free quarks and the distribution for a quark of color i would be

$$G_{q_i/p}^{(0)}(x) = \delta(x - \frac{1}{3}). \quad (2.10)$$

By putting in minimally connected gluon exchange diagrams, as in Brodsky and Farrar,⁹ we modify this distribution to a form which obeys the constituent counting rules. If we still require at this level of approximation that all the momentum is

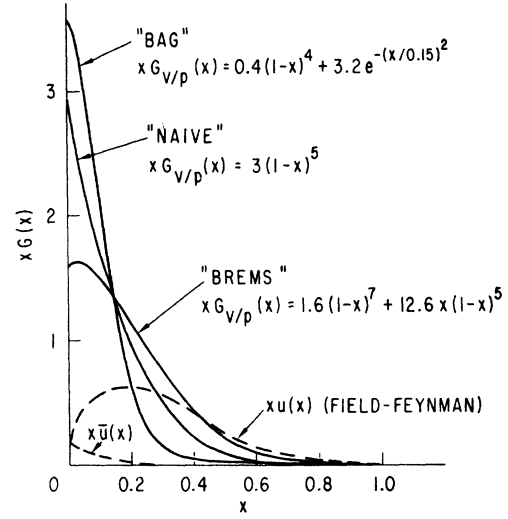


FIG. 1. The three models for gluon distributions discussed in the text are displayed and compared with the parametrization of Field and Feynman, Ref. 3, for a valence-quark and a sea-antiquark distribution.

carried by the three valence quarks, we can write an "improved" form

$$G_{q_i/p}^{(1)}(x) = 20x(1-x)^3, \quad (2.11)$$

where the normalization is fixed by

$$\int_0^1 G_{q_i/p}^{(1)}(x) dx = 1, \quad (2.12)$$

$$\int_0^1 x G_{q_i/p}^{(1)}(x) dx = \frac{1}{3}.$$

We can now take into account the probability that one of the valence quarks can emit a virtual gluon through an internal "Bremsstrahlung" mechanism. We again invoke the form of the constituent counting rules to approximate the "irreducible" distribution of quarks and gluons as

$$\begin{aligned} g_{V_j^i/q_i}^{(1)}(x) &\cong \beta(1-x), \\ g_{q_j/q_i}^{(1)}(x) &\cong \beta(1-x), \end{aligned} \quad (2.13)$$

where $V_j^i = \sum T_{ij}^a V_a$, with the T_{ij}^a , defined in Appendix B, is the gluon which changes color i to color j . We can now write a second-level approximation where the proton contains both quarks and gluons,

$$G_{V_j^i/p}^{(2)}(x) \cong \int_x^1 dy g_{V_j^i/q_i}^{(1)}(x/y) G_{q_i/p}^{(1)}(y) \quad (2.14)$$

$$G_{q_i/p}^{(2)}(x) \cong \eta G_{q_i/p}^{(1)}(x) + \sum_j \int_x^1 dy g_{q_i/q_j}^{(1)}(x/y) G_{q_j/p}^{(1)}(y). \quad (2.15)$$

With the forms (2.12) and (2.13) the integrals can

be evaluated exactly to give

$$\begin{aligned} G_{v_j^i/p}^{(2)}(x) &\cong \beta(1-x)^5, \\ G_{q_i/p}^{(2)}(x) &\cong 20\eta x(1-x)^3 + \frac{8}{3}\beta(1-x)^5. \end{aligned} \quad (2.16)$$

Conservation of momentum gives the constraint $\eta \cong 1 - 8\beta/21$. One of the limitations of this simple approach is that if β is too large we will have $\eta < 0$ and we will be able to find a range in which $G_{q_i/p}(x) < 0$.

We do not yet have any antiquarks in the proton. At the next level of approximation we can allow a gluon to create a $q\bar{q}$ pair or to form another gluon by bremsstrahlung. The constituent counting rules allow us to write

$$g_{q_i/v_j^i}^{(1)}(x) = g_{\bar{q}_i/v_j^i}^{(1)}(x) = \beta(1-x) \quad (2.17)$$

and

$$g_{v_j^i/v_j^i}^{(1)}(x) = (\delta_j^k + \delta_i^j)\beta(1-x). \quad (2.18)$$

where δ_j^k is the Kronecker δ . This gives still another level of complexity to our proton distribution functions,

$$G_{\bar{q}_i/p}^{(3)}(x) \cong \sum_i \int_x^1 dy g_{\bar{q}_i/v_j^i}^{(1)}(x/y) G_{v_j^i/p}^{(2)}(y), \quad (2.19)$$

$$\begin{aligned} G_{v_j^i/p}^{(3)}(x) &\cong \gamma G_{v_j^i/p}^{(2)}(x) + \sum_{k,l} \int_x^1 dy g_{v_j^i/v_k^l}^{(1)}(x/y) G_{v_k^l/p}^{(2)}(y) \\ &\quad + \int_x^1 dy g_{v_j^i/q_i}^{(1)}(x/y) G_{q_i/p}^{(2)}(y), \end{aligned} \quad (2.20)$$

$$\begin{aligned} G_{q_i/p}^{(3)}(x) &\cong \eta G_{q_i/p}^{(2)}(x) + \sum_j \int_x^1 dy g_{q_i/v_j^i}^{(1)}(x/y) G_{v_j^i/p}^{(2)}(y) \\ &\quad + \sum_j \int_x^1 dy g_{q_i/q_j}^{(1)}(x/y) G_{q_j/p}^{(2)}(y). \end{aligned} \quad (2.21)$$

Inserting (2.17) and (2.16) into (2.19) yields

$$\begin{aligned} G_{\bar{q}_i/p}^{(3)}(x) &= \frac{8}{3}\beta^2 \frac{(1-x)^6}{6} \\ &\quad \times [1 - x {}_2F_1(6, 1; 7; 1-x)]. \end{aligned} \quad (2.22)$$

However, in the spirit of the approximations being considered here we replace the hypergeometric function by an asymptotic form

$$x {}_2F_1(6, 1; 7; 1-x) \cong 1 - \frac{1}{7} \frac{(x-1)}{x} + \dots \quad (2.23)$$

This gives

$$G_{\bar{q}_i/p}^{(3)}(x) \cong \left(\frac{8}{3}\right) \frac{\beta^2}{42} \frac{(1-x)^7}{x}, \quad (2.24)$$

$$\begin{aligned} G_{v_j^i/p}^{(3)}(x) &\cong (\gamma\beta + \beta\eta)(1-x)^5 \\ &\quad + \left[\frac{16}{3}\beta^2 + \frac{8}{3}\beta^2\right] \frac{1}{42} \frac{(1-x)^7}{x}, \end{aligned} \quad (2.25)$$

$$\begin{aligned} G_{q_i/p}^{(3)}(x) &\cong 20\eta^2 x(1-x)^3 + \frac{16}{3}\eta\beta(1-x)^5 \\ &\quad + \left[\frac{8}{3} + \left(\frac{8}{3}\right)^2\right] \frac{\beta^2}{42} \frac{(1-x)^7}{x}, \end{aligned} \quad (2.26)$$

with momentum conservation giving the constraint $\gamma \cong 1 - \frac{77}{84}\beta$. Again, these expressions can only be valid for small values of β . Two things we might extract from (2.24) and (2.25) are the ratio of the color-singlet distributions near $x=0$,

$$\lim_{x \rightarrow 0} \left(\sum_{ij} G_{v_j^i/p}^{(3)}(x) \right) / \left(\sum_j G_{\bar{q}_j/p}^{(3)}(x) \right) = 8, \quad (2.27)$$

and the approximate form

$$\sum_{ij} G_{v_j^i/p}^{(3)}(x) \cong a(1-x)^5 + b \frac{(1-x)^7}{x}. \quad (2.28)$$

If we extract from the Field-Feynman parametrization the condition

$$G_{\bar{u}/p}(x) \rightarrow \frac{0.2}{x}, \quad x \rightarrow 0 \quad (2.29)$$

Then (2.27) and (2.28) suggest the form

$$G_{v/p}(x) \cong 12.6(1-x)^5 + 1.6 \frac{(1-x)^7}{x}, \quad (2.30)$$

which is normalized using (2.4). This form is also plotted in Fig. 1 and we will use it in our calculations.

A virtue of this exercise is that, in addition to providing another concrete model for our calculations, it roughly demonstrates the relation between the shape of the valence-quark distribution, the gluon distribution, and the sea-anti-quark distribution in a model with interactions between gluons and quarks.

Bag-bremsstrahlung model for $G_{v/p}(x)$

Another possible gluon distribution, suggested by Politzer,^{11,7} has two components. One component corresponds to bremsstrahlung of gluons from valence quarks. In this model, if a valence-quark distribution is approximated by

$$xG_{q/p}(x) \cong a(1-x)^3, \quad (2.31)$$

then the resulting gluons would have a distribution

$$\begin{aligned} xG_{v/p}^{(1)}(x) &\cong \frac{\alpha_s}{\pi} a(1-x)^4 \\ &\cong 0.15 a(1-x)^4. \end{aligned} \quad (2.32)$$

The other (much larger) component comes from the "bag" which we assume is made out of gluons. If the bag diameter is ~ 1.4 fm then the momentum-space distribution will have width $\Delta p/p \approx 0.15$, where we have assumed that there is no structure in the bag (i.e., that it is as smooth as possible). Thus motivated, we parametrize the gluon distribution as

$$xG_{v/p}(x) = 0.4(1-x)^4 + 3.2e^{-(x/0.15)^2}, \quad (2.33)$$

where the normalization of the Gaussian is de-

terminated by the momentum integral condition (2.4). This gluon distribution is also shown in Fig. 1. In this picture, the sea quarks would also have a two-component distribution, but the power-law tail in this case would be very tiny indeed.

One virtue of this model for the gluonic content of the proton is that, in a sense, it represents an extreme; the gluons have been made as soft as possible. In the context of a hard-scattering model, then, (2.33) may be thought of as yielding a minimal gluonic contribution to the hadronic process which is being calculated.

In general, we wish to avoid being dogmatic about how gluons are distributed in the proton. We believe that the distributions we will use in our calculation with the hard-scattering model, (2.8), (2.29), and (2.33), represent a reasonable variation in shape for this function. We are aware that the arguments we have presented here involve a good deal of guesswork. An attractive alternative is that gluon distributions might be inferred from data on the process $p\bar{p} \rightarrow (\psi + \gamma)X$. As discussed by Einhorn and Ellis,¹² this would be possible if the dominant production mechanism were $VV \rightarrow \chi$ ($\chi = \text{even-}C, c\bar{c}$ state) followed by the decay $\chi \rightarrow \psi\gamma$. A specific calculation in the framework of QCD which attempts to understand the shape of the gluon distribution has been discussed by Novikov *et al.*¹³

Gluon decay distributions

The final piece of guesswork we must do concerns the function $D_{\pi^0/\nu}(z)$, which represents the probability that a gluon jet gives a fraction z of its momentum to a pion. We would not need to know $D_{\pi^0/\nu}(z)$ if we were content to calculate and compare with data for jet cross sections. However, the best data from the CERN ISR at this time are for single-particle inclusive cross sections, and this will probably continue to be true in the future. The extra "uncertainty" in our calculation attributable to including this function is probably small compared to the experimental difficulties in measuring an appropriate jet cross section.

We proceed as follows: We estimate that, as with quark jets, approximately $\frac{3}{5}$ of the momentum of the gluon will eventually be carried by pions. Because the gluon is a flavor isosinglet, this momentum should be equally distributed among π^0 , π^+ , and π^- , at least as $z \rightarrow 1$. The remaining $\frac{2}{5}$ of the momentum will be allocated to K 's and baryon-antibaryon pairs in a way which need not concern us here. A simple ansatz suggested by the constituent-counting rules is

$$D_{\pi^0/\nu}(z) = \left(\frac{4}{5}\right) \frac{(1-z)^3}{z} . \quad (2.34)$$

In order to test the calculation for sensitivity to the form of the gluon decay function, we have also calculated with the distribution

$$D_{\pi^0/\nu}(z) = \frac{(1-z)^4}{z} . \quad (2.35)$$

The results we will present in Sec. IV are quite insensitive to which of these forms we use, and we will only present calculations using (2.34).

It is interesting to note here that gluon decay functions may be experimentally accessible. If current interpretations of the Okubo-Zweig-Iizuka-rule-violating decays of the even- C charmonium states χ are correct, the decays $\chi \rightarrow \text{hadrons}$ can be viewed as proceeding through an intermediate two-gluon mode. The distribution of hadrons in the variable $z_h = 2E_h^*/m_\chi$ could therefore give an indication of the shape of $D_{\pi^0/\nu}(z)$.

III. SPIN SUMS AND GAUGE INVARIANCE FOR GLUON CROSS SECTIONS

In order to deal with processes involving the scattering of colored vector gluons within the framework of the parton model, we need to know the quark-gluon and gluon-gluon scattering cross sections. The lowest-order amplitudes for these processes are easily obtained from the Feynman rules of the gauge theory,¹⁴ and are given in Appendix A. We encounter, however, a technical difficulty when we attempt to square the amplitudes and perform the spin sums using standard trace techniques. The origin of this problem involves how we choose to deal with the longitudinal polarizations of the gluons in the proton.

We interpret the hard-scattering parton model as being valid when the internal scattering process is treated as if it involves on-mass-shell particles.¹⁵ We therefore calculate our cross sections for massless gluons and massless quarks. Specifically, this means that our gluons are assumed to have only transverse polarizations.

Quark-gluon scattering

Let us see what this implies for the process $q(p_1)V(q_1) \rightarrow q(p_2)V(q_2)$, where we temporarily suppress color degrees of freedom. The amplitude given in Eqs. (A10)–(A12) is of the form

$$\mathfrak{M} = T_{\mu\nu} \epsilon_1^\mu \epsilon_2^\nu , \quad (3.1)$$

where ϵ_1 and ϵ_2 are the polarization vectors of the gluons. One can easily verify the gauge invariance of the amplitude by checking that

$$T_{\mu\nu} \epsilon_1^\mu q_2^\nu = 0 . \quad (3.2)$$

However, when we square the amplitude and sum (average) over final (initial) spins,

$$\langle |\mathfrak{M}|^2 \rangle = \frac{1}{4} \sum_{\text{spins}} T_{\mu\nu} T_{\mu'\nu'}^* \epsilon_1^\mu \epsilon_1^{*\mu'} \epsilon_2^\nu \epsilon_2^{*\nu'} , \quad (3.3)$$

we must *not* make the ‘‘Feynman gauge’’ replacement

$$\sum_{\text{spins}} \epsilon_1^\mu \epsilon_1^{*\mu'} \rightarrow -g^{\mu\mu'} , \quad (3.4)$$

as is commonly done in QED calculations. This replacement introduces unwanted longitudinal components into the polarization vector and, unlike the case of QED, these components do not vanish unless there is only one external gluon. One way to obtain the correct, gauge-invariant, cross section is to use the appropriate projection operators for the transverse polarization states in the scattering process,¹⁶

$$\sum_{\text{spins}} \epsilon_1^\mu \epsilon_1^{*\mu'} = -g^{\mu\mu'} + \frac{2}{s} (p_1^\mu q_1^{\mu'} + p_1^{\mu'} q_1^\mu) , \quad (3.5)$$

$$\sum_{\text{spins}} \epsilon_2^\nu \epsilon_2^{*\nu'} = -g^{\nu\nu'} + \frac{2}{s} (p_2^\nu q_2^{\nu'} + p_2^{\nu'} q_2^\nu) . \quad (3.6)$$

[Actually, because of (3.2) we need only use (3.5) or (3.6) for one of the spin sums and may use (3.4) for the other.]

The result is

$$\begin{aligned} \langle |\mathfrak{M}|^2 \rangle &= 1 - \frac{4}{9} \frac{u}{s} - \frac{4}{9} \frac{u}{s} - \frac{2us}{t^2} \\ &= \langle |\mathfrak{M}|^2 \rangle_{\mathcal{F}} + \frac{1}{2} \frac{us}{t^2} , \end{aligned} \quad (3.7)$$

where $\langle |\mathfrak{M}|^2 \rangle_{\mathcal{F}}$ is the (incorrect) result obtained using (3.4).

Another way to obtain the correct result is to introduce the Fadeev Popov ghost in the following way. As indicated in Fig. 2 the modulus squared of the t -channel amplitude can be identified through unitarity with a cylinder. The replacement (3.4) corresponds to evaluating all gluon lines in the cylinder in the Feynman gauge. The Feynman rules of the theory¹⁴ then tell us that we can remove the unwanted longitudinal polarization by introducing ghost loops into the calculation as shown schematically in Fig. 2.

The two cylinders containing ghosts are easily



FIG. 2. Schematic indication of how unwanted longitudinal polarization of physical gluons which appear in certain gauges can be removed by introducing ghost loops.

evaluated to yield

$$\begin{aligned} \langle |\mathfrak{M}|^2 \rangle_{\text{ghost loops}} &= \left(\frac{1}{4}\right) \left(\frac{1}{2}\right) (-2) \frac{1}{t^2} \text{Tr}(\not{p}_1 \not{q}_2 \not{p}_2 \not{q}_1) \\ &= \frac{1}{2} \frac{us}{t^2} , \end{aligned} \quad (3.8)$$

so that

$$\langle |\mathfrak{M}|^2 \rangle = \langle |\mathfrak{M}|^2 \rangle_{\mathcal{F}} + \langle |\mathfrak{M}|^2 \rangle_{\text{ghost loops}} , \quad (3.9)$$

which is equivalent to (3.7). We should emphasize that this is only a formal technique to evaluate (3.3) for on-shell quark-gluon scattering. We are *not* introducing a ghost component into the proton wave function.

Gluon-gluon scattering

We can now look at the same problem in the process $VV \rightarrow VV$, which has an amplitude of the form

$$\mathfrak{M} = T_{\lambda\mu\nu\sigma} \epsilon_1^\lambda \epsilon_2^\mu \epsilon_3^\nu \epsilon_4^\sigma , \quad (3.10)$$

as given in Eqs. (A24)–(A27) in Appendix A. One can again show that the amplitude is gauge invariant, so that

$$T_{\lambda\mu\nu\sigma} q_1^\lambda \epsilon_2^\mu \epsilon_3^\nu \epsilon_4^\sigma = 0 . \quad (3.11)$$

The spin-averaged gauge-invariant squared amplitude

$$\begin{aligned} \langle |\mathfrak{M}|^2 \rangle &= \left(\frac{1}{4}\right) \sum_{\text{spins}} T_{\lambda\mu\nu\sigma} T_{\lambda'\mu'\nu'\sigma'}^* \\ &\quad \times \epsilon_1^\lambda \epsilon_1^{*\lambda'} \epsilon_2^\mu \epsilon_2^{*\mu'} \epsilon_3^\nu \epsilon_3^{*\nu'} \epsilon_4^\sigma \epsilon_4^{*\sigma'} , \end{aligned} \quad (3.12)$$

can again be evaluated using the projection operators analogous to (3.5) and (3.6) for (at least three of) the spin sums. This procedure, however involves evaluating a great many terms (228 420, to be precise). This is an inconveniently large task even for the algebraic-manipulation program¹ ASHMEDAI (which we use to evaluate some of the spin sums in the ‘‘Feynman gauge’’). In this case the ghost-cylinder algorithm indicated schematically in Fig. 3 is much more efficient. Figure 3 displays the eight distinct cylinders for the modulus squared of the t -channel graph. Each ghost loop can have two directions, so cylinder (d), for example, represents four separate graphs. The result is

$$\begin{aligned} \langle |\mathfrak{M}_t|^2 \rangle &= \frac{9}{8} \left(\frac{17}{2} - 4 \frac{us}{t^2} \right) \\ &= \langle |\mathfrak{M}_t|^2 \rangle_{\mathcal{F}} + \frac{9}{8} \left(-\frac{1}{8} + \frac{9}{4} \frac{us}{t^2} \right) , \end{aligned} \quad (3.13)$$

where $\langle |\mathfrak{M}_t|^2 \rangle_{\mathcal{F}}$ represents the answer found calculating the gluon cylinder in the Feynman gauge. The interference terms between gluon exchange in different channels are typified by $\mathfrak{M}_i \mathfrak{M}_j^*$. Using

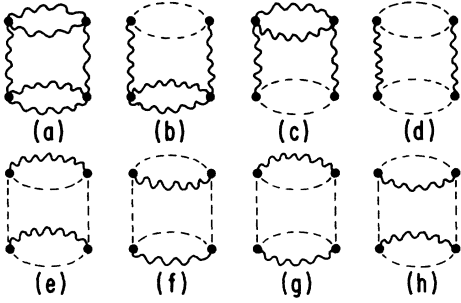


FIG. 3. The eight distinct unitarity cylinders for $|\mathfrak{N}_f^2|$ in $VV \rightarrow VV$. Each ghost loop can have two directions.

unitarity, this can be represented by a tetrahedron, and Fig. 4 shows the eight distinct tetrahedral diagrams which can be drawn. As each ghost loop has two possible directions, these diagrams represent 15 distinct terms. The result is

$$\begin{aligned} \langle 2\mathfrak{N}_f \mathfrak{N}_u^* \rangle &= \frac{9}{16} \left(15 - \frac{s^2}{tu} \right) \\ &= \langle 2\mathfrak{N}_f \mathfrak{N}_u^* \rangle_F - \frac{9}{16} \left(\frac{1}{4} \frac{s^2}{tu} \right). \end{aligned} \quad (3.14)$$

The complete answer for gluon-gluon scattering is then given in Eqs. (A28)–(A35) in Appendix A.

We note here that other methods for dealing with the spin of the gluons are possible. We might, for example, give the gluons some effective mass, μ^2 , and calculate as if they were massive particles with three spin projections. As discussed by Dombey and Vayonakis,¹⁸ this method does not limit smoothly to the zero-mass case as $\mu^2 \rightarrow 0$. Alternatively, we could make separate models for the transverse and longitudinal distributions of virtual gluons in the proton and compute separate cross sections. Both of these methods would add considerable complexity to the calculations and introduce additional freedom into the answer. Aside from the fact that our method adheres most

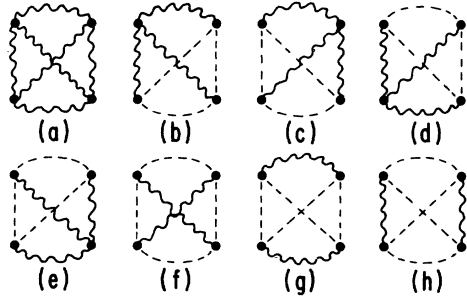


FIG. 4. The eight distinct unitarity tetrahedra for $2\mathfrak{N}_f \mathfrak{N}_u^*$ in $VV \rightarrow VV$. Each ghost loop can have two directions.

closely to the original formulation of the hard-scattering parton model, it is the simplest and least ambiguous calculation we can make. Moreover, these alternative approaches will presumably differ from our result by an amount comparable to $\langle |\mathfrak{N}_f|^2 \rangle - \langle |\mathfrak{N}_f|^2 \rangle_F$, which is a small correction to the results we present.

The problem of the spin degrees of freedom of vector partons has been discussed in another context by Elias *et al.*¹⁹

IV. GLUONS AND QUARKS IN THE HARD-SCATTERING MODEL

The calculation

We are now prepared to calculate the inclusive cross section $Ed\sigma/d^3p(pp \rightarrow \pi^0 X)$ at large p_T in the framework of the hard-scattering model defined by Eq. (2.1). We take an incoherent sum over the internal processes $qq \rightarrow qq$, $q\bar{q} \rightarrow qq$, $\bar{q}\bar{q} \rightarrow \bar{q}\bar{q}$, $qV \rightarrow qV$, $\bar{q}V \rightarrow \bar{q}V$, $q\bar{q} \rightarrow VV$, $VV \rightarrow q\bar{q}$, and $VV \rightarrow VV$ which can contribute an approximately scale-invariant piece to the cross section. The color-averaged, spin-averaged cross section is calculated to leading order in perturbation theory as described in Sec. III and Appendix A. In these cross-section formulas we use a renormalization-group-improved form for the quark-gluon coupling $\alpha_s = g_s^2/4\pi$, and we take a *range* for this coupling,

$$\alpha_s^{\max}(Q^2) = \frac{0.50}{1 + 0.36 \ln(Q^2/4)}, \quad (4.1)$$

$$\alpha_s^{\min}(Q^2) = \frac{1}{2} \alpha_s^{\max}(Q^2),$$

where Q^2 is the “exchange” momentum transfer. The motivation for choosing this range is discussed in Ref. 6.

For those processes involving quarks we use the Field-Feynman³ parametrization of the $G_{q/p}(x)$ and $D_{\tau/q}(z)$. For the gluons we consider a choice of [(2.8)—naive], [(2.29)—bremis], or [(2.33)—bag] for $G_{v/p}(x)$ and use (2.34) for $D_{\tau/v}(z)$.

Figure 5 shows the calculated inclusive cross section for $pp \rightarrow \pi^0 X$ at $\sqrt{s} = 53$ GeV, $\theta = 90^\circ$, which results when $G_{v/p}$ is given by [(2.29)—bremis]. Also shown are the ISR data^{20,21} at this energy and the Field-Feynman fit to these data. To approximately account for the effect of p_T -smearing within the G 's we have shifted our curves by

$$\begin{aligned} p_T &\rightarrow p_T + \langle |p_T| \rangle, \\ \langle |p_T| \rangle &= 0.3 \text{ GeV}. \end{aligned} \quad (4.2)$$

This corresponds to a minimal p_T -smearing. The same comparison is made for $G_{v/p}$ given by [(2.33)—bag] in Fig. 6 with the quark distributions held the same. The remaining model for $G_{v/p}$,

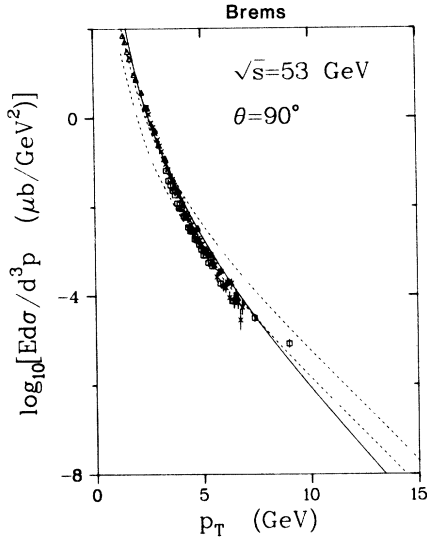


FIG. 5. Inclusive cross section for pion production, $E d\sigma/d^3p (pp \rightarrow \pi X)$, versus p_T at $\sqrt{s} = 53$ GeV, $\theta = 90^\circ$. The data are $pp \rightarrow \pi^0 + X$ from Ref. 20 (triangles) and Ref. 21 (squares) and $pp \rightarrow (\pi^+ + \pi^-)/2 + X$ from Ref. 21 (crosses). The solid curve is calculated from the model of Field and Feynman (Ref. 3). The dashed curves are the results of our QCD calculation using the range of $\alpha_s(Q^2)$ parameterized in Eq. (4.1). Both models use the Field-Feynman quark distributions, and the QCD curves use gluon distribution given by [(2.29)—brems].

[(2.8)—naive], is intermediate between these p_T distributions.

Two things are notable about these comparisons:

(1) The normalizations of the calculations are *not* arbitrary. The running coupling constant defined by (4.1) is small over the important range of momentum transfer. The fact that we agree approximately with the normalization of the data is therefore significant. We have started out with the hypothesis that a perturbative calculation in QCD could provide a rough guide to large-momentum-transfer data. If we were drastically below (or above) the data, it would indicate the need for large corrections and it would be unlikely that a perturbation theory approach would be valid. Recall that efforts to ascribe these large- p_T data to a single mechanism such as $qq \rightarrow qq$ (Refs. 2–5) or $qM \rightarrow qM$ (Ref. 22) involve fitting to the data with a function of undetermined normalization. If we were to characterize these models by effective couplings, then the coupling constants would, in general, be large and have no discernible relationship to the QCD coupling inferred from other reactions.

(2) There is a rather gentle crossover between the curves in our calculation and the Field-Feynman model. We do not necessarily expect at this energy an obvious p_T^{-4} component to the cross sec-

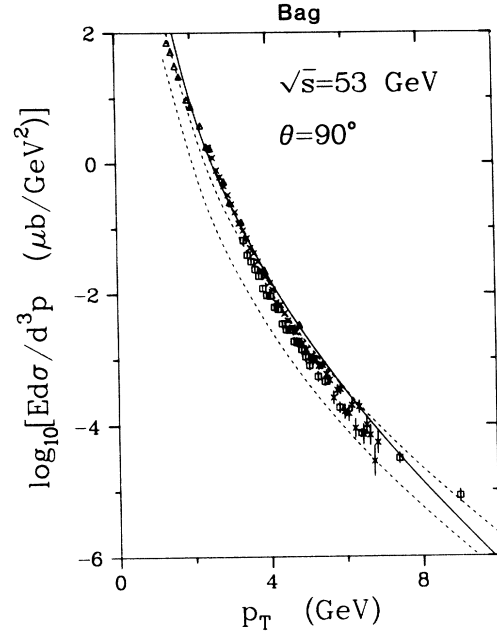


FIG. 6. Inclusive cross section for pion production, $E d\sigma/d^3p (pp \rightarrow \pi X)$, versus p_T at $\sqrt{s} = 53$ GeV, $\theta = 90^\circ$. The data are the same as in Fig. 5. The solid curve is calculated using the Field and Feynman parametrization of $d\sigma/d\hat{t}$. The dashed curves are the results of our QCD calculation using the range of $\alpha_s(Q^2)$ parameterized in Eq. (4.1). Both models use the Field-Feynman quark distributions, and the QCD curves use gluon distributions given by [(2.33)—bag].

tion for higher values of p_T . If we allow for scaling violations in the G 's and D 's,⁶ it may even be possible to remove completely this crossover. However, it may also be possible to attribute an excess of events over the extrapolation of the Field-Feynman curve as some evidence for this type of scale-invariant scattering mechanism. The resolution of this issue awaits more intricate calculations and data at higher p_T .

It is interesting to see what the relative strengths are of the various internal mechanisms ($qq \rightarrow qq$, $qV \rightarrow qV$, etc.). We show in Fig. 7 the fraction of the inclusive cross section resulting from each process as a function of p_T . These quantities are fairly sensitive to how we choose $G_{V/p}$ and we show the results of all three models. In all cases, if p_T is small enough then the process $qV \rightarrow q$ contributes significantly to the cross section. (The notation indicates that the internal mechanism is $qV \rightarrow qV$ and that the scattered quark fragments to produce the observed π .) Because we have assumed that gluons give less momentum to a π when they fragment, the contribution from $qV \rightarrow V$ at a given p_T is less than that of $qV \rightarrow q$. The proportion of particles attributable to $qq \rightarrow q$ grows

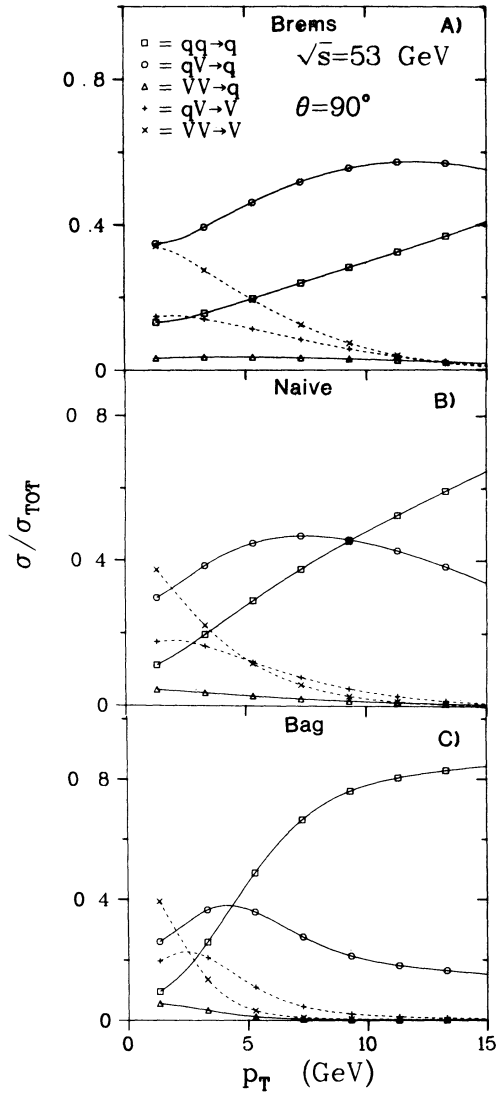


FIG. 7. Contribution of various subprocesses to the inclusive cross section $E d\sigma/d^3p (pp \rightarrow \pi X)$. The notation $qV \rightarrow q$ refers to the internal process $qV \rightarrow qV$ where the observed hadron comes from the quark. No distinction is made here between quarks and antiquarks. The gluon distributions used are (A) [(2.39)—brems], (B) [(2.8)—naive], (C) [(2.33)—bag].

steadily with p_T in our calculation.

If we go to higher energies so that we can achieve high p_T while staying at comparatively low values of $x_T = 2p_T/\sqrt{s}$, the effect of adding gluon scattering mechanisms into the hard-scattering model can be quite dramatic. As shown in Fig. 8, the expectation from our QCD perturbation theory calculation at $\sqrt{s} = 800$ GeV is more than two orders of magnitude greater at $p_T = 15$ GeV than an extrapolation based on the Field-Feynman model. This curve is completely normalized and can be

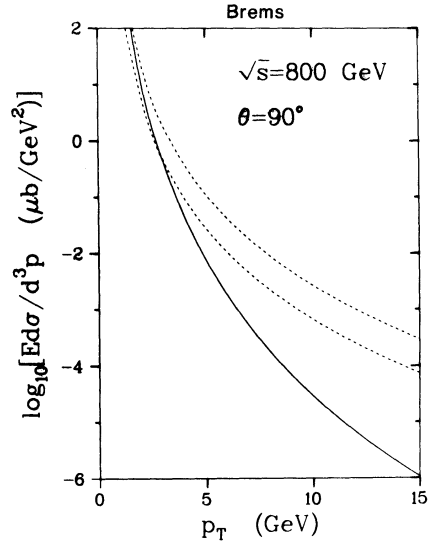


FIG. 8. Inclusive cross section for pion production, $E d\sigma/d^3p (pp \rightarrow \pi X)$, versus p_T at $\sqrt{s} = 800$ GeV, $\theta = 90^\circ$. The solid curve is calculated using the Field and Feynman parametrization of $d\sigma/d\hat{t}$. The dashed curves are the results of our QCD calculation using the range of $\alpha_s(Q^2)$ parametrized in Eq. (4.1). Both models use the Field-Feynman quark distributions, and the QCD curves use gluon distributions given by [(2.29)—brems].

used, for example, to compare with data inferred from cosmic-ray experiments, where it is claimed²³ that there is evidence for a p_T^{-4} cross section. At these high values of \sqrt{s} the calculation is quite insensitive to the exact form used for G_V/p . We use [(2.29)—brems] to make these curves. In Fig. 9 we show the relative strengths of the internal processes at $p_T = 10$ GeV for two choices of G_V/p , the bag and the bremsstrahlung distributions. The contribution from $qq - qq$ is quite small at these low values of x_T . In Fig. 10 we show jet cross sections at $\sqrt{s} = 800$ GeV obtained by making the substitution $D_{r/c}(z) = \delta(1-z)$ in (2.1).

Comments

We want to emphasize again that this calculation is not intended to be a fit to currently available large- p_T data. Rather, it is an attempt to calculate in a straightforward manner what should be expected for large- p_T hadronic production if the lowest order of perturbation theory is a guide to QCD at large momentum transfer. Although there is some guesswork involved in picking the gluon structure functions nevertheless there are no free parameters. However, we are quite aware that there are higher-order corrections which we are not calculating, and which could be quite significant, particularly at ISR energies or below. Bearing this in mind, we consider the excellent agreement between the upper curve in Fig. 6 and

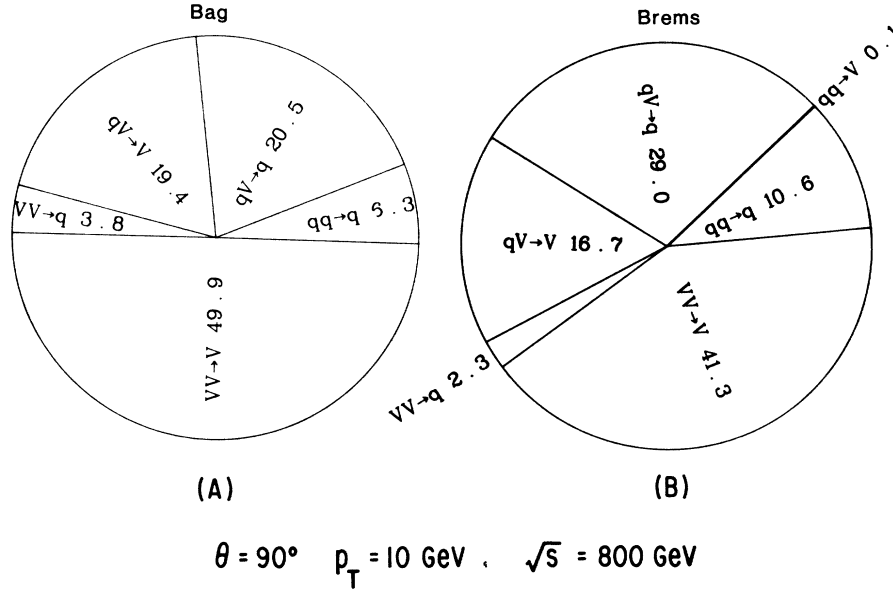


Fig. 9. Contribution of various subprocesses to the inclusive cross section $E d\sigma/d^3p$ ($pp \rightarrow \pi X$). In the notation used, $qV \rightarrow q$ refers to a process where $qV \rightarrow qV$ and the observed hadron comes from the quark. No distinction is made here between quarks and antiquarks. The gluon distributions used are (A) [(2.33)—bag], (B) [(2.29)—brems].

the data to be somewhat accidental. We certainly do not think that we have achieved an overall fit to the ISR data, for were we to make this claim, we would swiftly discover that our s dependence is wrong.

Let us speculate on the elements which might

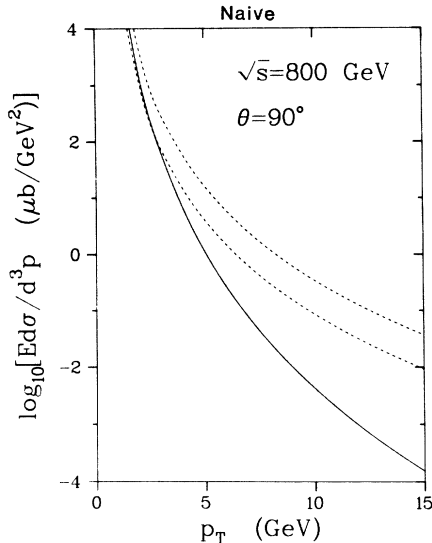


FIG. 10. Inclusive cross section for jet production, $E d\sigma/d^3p$ ($pp \rightarrow jet + X$), versus p_T at $\sqrt{s} = 53$ GeV, $\theta = 90^\circ$. The solid curve is calculated using the Field and Feynman parametrization of $d\sigma/d\hat{t}$. The dashed curves are the results of our QCD calculation using the range of $\alpha_s(Q^2)$ parametrized in Eq. (4.1). Both models use the Field-Feynman quark distributions, and the QCD curves use gluon distributions given by [(2.8)—naive].

be necessary to attempt a complete fit to the data. We cannot at the present time answer the question of why the data look more like p_T^{-8} than p_T^{-4} , but we can say the following:

(1) Recent data may indicate that the use of the hard-scattering model is justifiable only when the elementary "partons" are treated as if they have a large mean transverse momentum.²⁴ This means that we might calculate with $G(x, k_T)$ and/or $D(x, k_T)$, where

$$\langle |k_T| \rangle \geq 0.5 \text{ GeV.}$$

A discussion of how this can change the shape of the p_T distribution can be found in the analysis of Feynman, Field, and Fox.²⁵ There are also hints^{26,27} that this k_T smearing could have a Q^2 dependence.

(2) We know that violations of naive Bjorken scaling occur in deep-inelastic processes. For processes involving leptons these can be empirically described^{6,28} by letting the quark distributions to Q^2 dependent,

$$G_{q/p}(x, Q^2) = G_{q/p}(x, Q_0^2) \times \exp \left[(0.2 - 0.9x) \ln \frac{Q^2}{Q_0^2} \right],$$

with $Q_0^2 \cong 3 \text{ GeV}^2$. There may be comparable Q^2 dependence in $G_{V/p}(x, Q^2)$, and conceivably also in the decay distributions $D_{r/q}(z, Q^2)$ and $D_{r/V}(z, Q^2)$.

(3) At some level one must find quasicohere processes, such as $qM \rightarrow qM$ [which appears in the constituent-interchange model (CIM)²²]. The ability to calculate these processes is probably outside

the limits of our perturbative approach, but there should be small- p_T ⁻⁸ corrections to our curves attributable to them.

Putting together all the freedom inherent in (1)–(3), it would seem possible to work out a fit to some subset of large- p_T data based roughly on the calculation reported above. However, we do not feel that it would be very instructive to do this without further theoretical input. There are certainly higher-order graphs in the perturbation expansion of QCD, and these graphs may contribute significant corrections to our lowest-order calculation. Recent theoretical analyses^{26, 27} indicate that these effects can result in scaling violations of the sort described above in (2), as well as a Q^2 -dependent k_T smearing in (1). This approach could conceivably lead to an overall understanding of high- p_T processes in the context of the QCD perturbation expansion. We have only taken the first step in that direction.

V. SIMPLE EXPERIMENTAL CONSEQUENCES AND CONCLUSION

The fact that gluons are flavor singlets enables us to predict, in kinematic regimes where the dominant process is $VV \rightarrow VV$, that one should find approximately equal production of π^+ , π^0 , and π^- . We can also note that the flavor content of the process $qV \rightarrow q$ (where we specify that it is the scattered quark which is producing the observed hadron) is to a first approximation the same as that of $qq \rightarrow q$. Combining these observations with our results in Sec. IV, we predict at ISR energies and below that particle ratios are roughly the same as those in the Field-Feynman (or any other) $qq \rightarrow qq$ model. At ISABELLE or Fermilab doubler-collider energies we should see approximate isospin independence over much of the available kinematic regime.

Beyond these simple qualitative observations we have little to say at this time. The details of particle ratios and quantum-number correlations depend on questions not adequately treated here. Since our calculation seems to indicate that gluon jets are produced copiously opposite a detected large- p_T hadron, we might speculate that these jets are different in some important way from the jets produced in $e^+e^- \rightarrow h$, $\mu p \rightarrow \mu hX$, or $\nu N \rightarrow \mu hX$. However, to enumerate just how they might be different is somewhat problematical. We have assumed, for example, that they are softer. There may indeed be some indications in Fermilab data²⁹ that away-side jets have a softer distribution of hadrons than toward-side jets.

Many predictions of this type, however, involve assumptions which are beyond the scope of this work. Higher-order corrections to QCD or hypo-

thetical nonperturbative effects may certainly change our results. Any calculation using perturbation theory must be suspect in that it does not explain the confinement of quarks and gluons which is presumably a feature of the complete theory. The possibility that infrared effects could modify substantially the Born approximation to large- p_T production has been discussed by many people.³⁰ A simple empirical model which does this has been discussed by Duke.³¹

Since calculations using the $qq \rightarrow qq$ mechanism alone would seem to indicate that a simple perturbation approach is inadequate in the regime where data are currently available, several people have constructed special models^{2-5, 22, 31} to account for the data. From our point of view some of these models have been rather poorly motivated in that they have not adequately dealt with the question of what suppresses the scattering of gluons. Since, as can be seen in Appendix A, the spin-averaged, color-averaged cross sections for $VV \rightarrow VV$ and $Vq \rightarrow Vq$ are large compared with $qq \rightarrow qq$ when calculated in perturbation theory, the assumption that $qq \rightarrow qq$ dominates must involve some sort of selective suppression of these gluon processes in nonperturbative calculations. At present we have no clue why there might be such a suppression.

Our goals have been more modest. We do not know that perturbation theory is right. It is merely too simple a possibility to overlook.

Note added in proof. It has come to our attention that the calculation of Combridge, Kripfganz, and Ranft³² for $|\mathfrak{M}^2(VV \rightarrow VV)|$ differs from ours by a small term ($\frac{9}{8}$)($\frac{1}{2}$). They use explicit polarization vectors instead of the ghost-subtraction procedure described in Sec. III. We suspect their calculation is correct, but we have not been able to find any error in ours. We thank B. Combridge for communicating their results to us prior to publication. None of our numerical results are sensitive to this.

ACKNOWLEDGMENTS

We are grateful for useful conversations with J. Babcock, S. Brodsky, W. Caswell, S. J. Chang, R. D. Field, and H. D. Politzer during the course of this research.

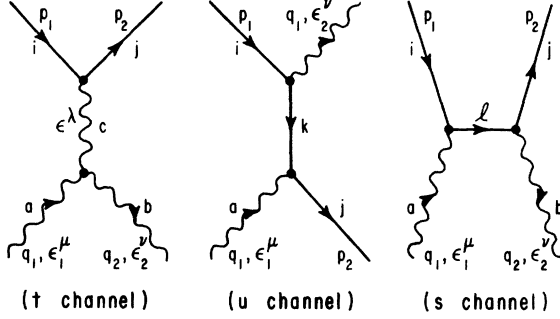
APPENDIX A: EVALUATION OF QCD GRAPHS

We include here expressions for the QCD processes we are considering, calculated to lowest order in the perturbation expansion. The Feynman rules we use are those given for massless quarks in Politzer's review¹⁴ and are shown in Fig. 11. The color sums are evaluated using techniques discussed in Appendix B, and the spin sums are discussed in Sec. III. The "Feynman gauge" is

$$\langle |\mathfrak{M}(q_\alpha \bar{q}_\beta \rightarrow q_\delta \bar{q}_\gamma)|^2 \rangle = g^4 \left\langle \frac{2}{9} \left[\delta_{\alpha\delta} \delta_{\beta\gamma} \frac{2(s^2 + u^2)}{t^2} + \delta_{\alpha\beta} \delta_{\gamma\delta} \frac{2(t^2 + u^2)}{s^2} + \delta_{\alpha\beta} \delta_{\beta\delta} \delta_{\delta\gamma} \left\langle -\frac{1}{3} \right\rangle \frac{4u^2}{st} \right] \right\rangle. \quad (\text{A8})$$

When calculating contributions to the hard-scattering model from $q\bar{q} \rightarrow q\bar{q}$, one must remember to sum over final-state flavors (e.g., $u\bar{u} \rightarrow u\bar{u}$, $u\bar{u} \rightarrow d\bar{d}$, etc.).

The process of $qV \rightarrow qV$.



(t channel) (u channel) (s channel)

$i, j, k, l = 1-3$ (quark color),

$a, b, c = 1-8$ (gluon color),

$\mu, \nu, \lambda =$ Lorentz indices,

$s = (p_1 + q_1)^2$, $t = (p_1 - p_2)^2$, $u = (p_1 - q_2)^2$.

Defining a Lorentz tensor which occurs in the three-gluon vertex,

$$C^{\mu\nu\lambda}(q_1, q_2, q_3) \equiv [(q_1 - q_2)^\nu g^{\mu\lambda} + (q_2 - q_3)^\mu g^{\nu\lambda} + (q_3 - q_1)^\lambda g^{\mu\nu}], \quad (\text{A9})$$

we suppress the flavor indices and write the invariant amplitudes for the three graphs shown above:

$$\mathfrak{M}_t(q_i V_a - q_j V_b) = \frac{g^2}{t} f^{cab} T_{ij}^c \epsilon_1^\mu \epsilon_2^\nu C_{\lambda\mu\nu}(q_1 - q_2, -q_1, q_2) \times \bar{u}_j(p_2) \gamma^\lambda u_i(p_1), \quad (\text{A10})$$

$$\mathfrak{M}_u(q_i V_a - q_j V_b) = -\frac{ig^2}{u} T_{ik}^b T_{kj}^a \bar{u}_j(p_2) \not{\epsilon}_1(\not{p}_1 - \not{q}_2) \not{\epsilon}_2 u_i(p_1), \quad (\text{A11})$$

$$\mathfrak{M}_s(q_i V_a - q_j V_b) = -\frac{ig^2}{s} T_{ii}^a T_{ij}^b \bar{u}_j(p_2) \not{\epsilon}_2(\not{p}_1 + \not{q}_1) \not{\epsilon}_1 u_i(p_1). \quad (\text{A12})$$

The spin and color sums yield

$$\langle |\mathfrak{M}_t(qV \rightarrow qV)|^2 \rangle = g^4 \left\langle \frac{1}{2} \right\rangle 4 \left(1 - \frac{us}{t^2} \right), \quad (\text{A13})$$

$$\mathfrak{M}(V_a V_b \rightarrow q_i q_j) = -g^2 \bar{u}_j(p_2) \left[T_{ik}^a T_{kj}^b \not{\epsilon}_2 \frac{(\not{q}_1 - \not{p}_1)}{t} \not{\epsilon}_1 + T_{ik}^b T_{kj}^a \not{\epsilon}_1 \frac{(\not{q}_2 - \not{p}_1)}{u} + if^{abc} T_{ij}^c \frac{\epsilon_1^\mu \epsilon_2^\nu \gamma^\lambda}{s} C_{\mu\nu\lambda}(-q_1, -q_2, q_1 + q_2) \right] v_i(p_1). \quad (\text{A21})$$

$$\langle |\mathfrak{M}_u(qV \rightarrow qV)|^2 \rangle = g^4 \left\langle \frac{2}{9} \right\rangle \left(-2 \frac{s}{u} \right), \quad (\text{A14})$$

$$\langle |\mathfrak{M}_s(qV \rightarrow qV)|^2 \rangle = g^4 \left\langle \frac{2}{9} \right\rangle \left(-2 \frac{u}{s} \right), \quad (\text{A15})$$

$$\langle 2\mathfrak{M}_t \mathfrak{M}_u^*(qV \rightarrow qV) \rangle = \left\langle \frac{i}{4} \right\rangle \left(-4i \frac{u}{t} \right), \quad (\text{A16})$$

$$\langle 2\mathfrak{M}_t \mathfrak{M}_s^*(qV \rightarrow qV) \rangle = \left\langle -\frac{i}{4} \right\rangle \left(4i \frac{s}{t} \right), \quad (\text{A17})$$

$$\langle 2\mathfrak{M}_u \mathfrak{M}_s^*(qV \rightarrow qV) \rangle = 0. \quad (\text{A18})$$

The two interference terms can be combined,

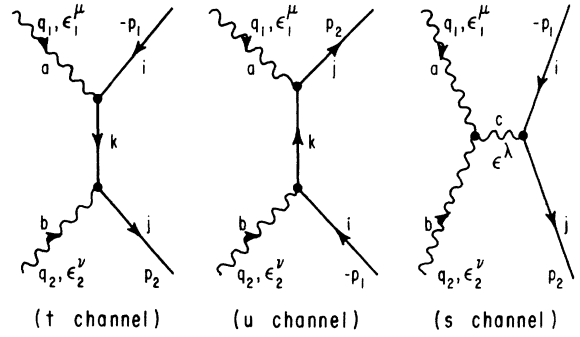
$$\langle 2\mathfrak{M}_t (\mathfrak{M}_u^* + \mathfrak{M}_s^*) \rangle = \frac{u+s}{t} = -1, \quad (\text{A19})$$

and so the cross section for $qV \rightarrow qV$ is

$$\frac{d\sigma}{dt}(qV \rightarrow qV) = \frac{g^4}{16\pi s^2} \left[2 \left(1 - \frac{us}{t^2} \right) - \frac{4}{9} \left(\frac{s}{u} + \frac{u}{s} \right) - 1 \right]. \quad (\text{A20})$$

The process $\bar{q}V \rightarrow \bar{q}V$. Time-reversal invariance implies that (A13)–(A20) also describe the process $\bar{q}V \rightarrow \bar{q}V$.

The process $VV \rightarrow q\bar{q}$.



(t channel) (u channel) (s channel)

$i, j, k = 1-3$ (quark color),

$a, b, c = 1-8$ (gluon color),

$\mu, \nu, \lambda =$ Lorentz indices,

$s = (q_1 + q_2)^2$, $t = (p_1 - q_2)^2$, $u = (p_1 - q_2)^2$.

The graphs for this process can be obtained from the $qV \rightarrow qV$ graphs by crossing, and so we adopt a more condensed notation. The invariant amplitude for $VV \rightarrow q\bar{q}$ is

Summing over spin and color yields

$$\begin{aligned} \langle |\mathfrak{M}(VV \rightarrow \bar{q}q)|^2 \rangle &= g^4 \left[\left\langle \frac{1}{12} \right\rangle \left(\frac{2tu}{t^2} \right) + \left\langle \frac{1}{12} \right\rangle \left(\frac{2tu}{u^2} \right) \right. \\ &\quad \left. - \left\langle \frac{3}{16} \right\rangle 4 \left(1 - \frac{ut}{s^2} \right) + \left\langle \frac{3}{32} \right\rangle 4 \right]. \end{aligned} \quad (\text{A22})$$

Comparing (A22) with the expression for $qV \rightarrow qV$ [(A20)], one sees that the different number of initial states averaged over has changed the normalization of each term by a factor of $\frac{3}{8}$, and that some terms have changed sign.

The process $q\bar{q} \rightarrow VV$. Except for the number of initial states averaged over, this process is the time reversal of $VV \rightarrow q\bar{q}$,

$$\begin{aligned} \langle |\mathfrak{M}(q\bar{q} \rightarrow VV)|^2 \rangle &= \frac{64}{9} \langle |\mathfrak{M}(VV \rightarrow q\bar{q})|^2 \rangle \\ &= g^{-4} \left[\left\langle \frac{16}{27} \right\rangle \left(\frac{2tu}{t^2} \right) + \left\langle \frac{16}{27} \right\rangle \left(\frac{2tu}{u^2} \right) \right. \\ &\quad \left. - \left\langle \frac{4}{3} \right\rangle 4 \left(1 - \frac{ut}{s^2} \right) + \left\langle \frac{2}{3} \right\rangle 4 \right]. \end{aligned} \quad (\text{A23})$$

The Lorentz tensors which can be contracted with $\epsilon^\lambda \epsilon^\mu \epsilon^\nu \epsilon^\sigma$ to form invariant amplitudes for the gluon-exchange diagrams are

$$\mathfrak{M}_t(V_a^\lambda V_b^\mu \rightarrow V_c^\nu V_d^\sigma) = -g^2 f_{aed} f_{ebc} C^{\lambda\tau\sigma}(-q_1, q_1 - q_4, q_4) (g_{\tau\tau}/t) C^{\tau\mu\nu}(q_2 - q_3, -q_2, q_3), \quad (\text{A24})$$

$$\mathfrak{M}_u(V_a^\lambda V_b^\mu \rightarrow V_c^\nu V_d^\sigma) = -g^2 f_{aec} f_{ebd} C^{\lambda\tau\nu}(-q_1, q_1 - q_3, q_3) (g_{\tau\tau}/u) C^{\tau\mu\sigma}(q_2 - q_4, -q_2, q_4), \quad (\text{A25})$$

$$\mathfrak{M}_s(V_a^\lambda V_b^\mu \rightarrow V_c^\nu V_d^\sigma) = -g^2 f_{dbe} f_{eca} C^{\lambda\mu\tau}(-q_1, -q_2, q_1 + q_2) (g_{\tau\tau}/s) C^{\tau\nu\sigma}(-q_3 - q_4, q_3, q_4). \quad (\text{A26})$$

For the four-point amplitude it is

$$\mathfrak{M}_4(V_a^\lambda V_b^\mu \rightarrow V_c^\nu V_d^\sigma) = -g^2 [f_{abe} f_{cde} (g^{\lambda\nu} g^{\mu\nu} - g^{\lambda\sigma} g^{\mu\nu}) + f_{ace} f_{bde} (g^{\lambda\mu} g^{\nu\sigma} - g^{\lambda\sigma} g^{\mu\nu}) + f_{ade} f_{cbe} (g^{\lambda\nu} g^{\mu\sigma} - g^{\lambda\mu} g^{\nu\sigma})]. \quad (\text{A27})$$

The spin and color sums yield

$$\langle |\mathfrak{M}_t(VV \rightarrow VV)|^2 \rangle = \left\langle \frac{9}{8} \right\rangle g^4 \left(\frac{17}{2} - 4 \frac{us}{t^2} \right), \quad (\text{A28})$$

$$\langle |\mathfrak{M}_u(VV \rightarrow VV)|^2 \rangle = \left\langle \frac{9}{8} \right\rangle g^4 \left(\frac{17}{2} - 4 \frac{st}{u^2} \right), \quad (\text{A29})$$

$$\langle |\mathfrak{M}_s(VV \rightarrow VV)|^2 \rangle = \left\langle \frac{9}{8} \right\rangle g^4 \left(\frac{17}{2} - 4 \frac{ut}{s^2} \right), \quad (\text{A30})$$

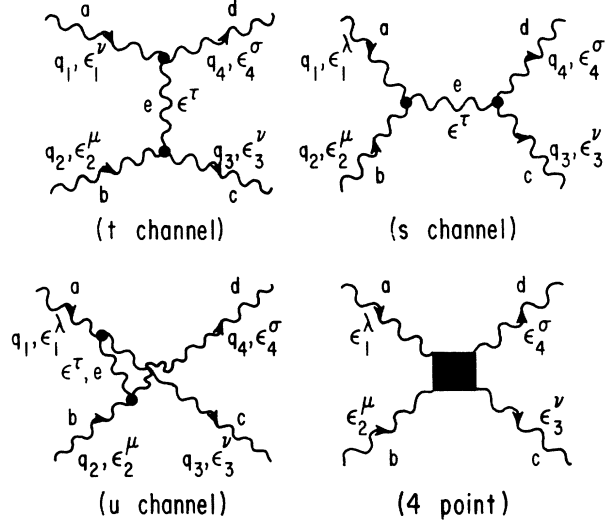
$$\langle |\mathfrak{M}_4(VV \rightarrow VV)|^2 \rangle = \left\langle \frac{9}{8} \right\rangle g^4 (27), \quad (\text{A31})$$

$$\langle 2\mathfrak{M}_t \mathfrak{M}_u^*(VV \rightarrow VV) \rangle = \left\langle \frac{9}{16} \right\rangle g^4 \left(15 - \frac{s^2}{tu} \right), \quad (\text{A32})$$

$$\langle 2\mathfrak{M}_t \mathfrak{M}_s^*(VV \rightarrow VV) \rangle = \left\langle \frac{9}{16} \right\rangle g^4 \left(15 - \frac{u^2}{ts} \right), \quad (\text{A33})$$

$$\langle 2\mathfrak{M}_u \mathfrak{M}_s^*(VV \rightarrow VV) \rangle = \left\langle \frac{9}{16} \right\rangle g^4 \left(15 - \frac{t^2}{us} \right), \quad (\text{A34})$$

The process $VV \rightarrow VV$.



with

$$s = (q_1 + q_2)^2 = (q_3 + q_4)^2, \quad t = (q_1 - q_4)^2 = (q_2 - q_3)^2,$$

$$u = (q_1 - q_3)^2 = (q_2 - q_4)^2,$$

$$C^{\mu\lambda\nu}(q_1, q_2, q_3) = [(q_1 - q_2)^\nu g^{\mu\lambda} + (q_2 - q_3)^\mu g^{\lambda\nu} + (q_3 - q_1)^\lambda g^{\mu\nu}].$$

$$\langle 2(\mathfrak{M}_t + \mathfrak{M}_u + \mathfrak{M}_s) \mathfrak{M}_4^*(VV \rightarrow VV) \rangle = 3 \left\langle \frac{9}{8} \right\rangle g^4 \left(-\frac{61}{4} \right). \quad (\text{A35})$$

Cross sections at 90° in the c.m. It is useful to compare the sizes of cross sections at 90° in the c.m., where $t = u = -s/2$. Defining $\alpha_s = (g^2/4\pi)$ in the usual way, we find

$$\frac{d\sigma}{dt} (q_\alpha q_\beta \rightarrow q_\alpha q_\beta) \Big|_{90^\circ} = \frac{\pi \alpha_s^2}{s^2} [2.22 + 1.04 \delta_{\alpha\beta}], \quad (\text{A36})$$

$$\begin{aligned} \frac{d\sigma}{dt} (q_\alpha \bar{q}_\beta \rightarrow q_\beta \bar{q}_\alpha) \Big|_{90^\circ} &= \frac{\pi \alpha_s^2}{s^2} [2.22 \delta_{\alpha\beta} \delta_{\beta\gamma} \\ &\quad + (0.22 + 0.15 \delta_{\alpha\beta}) \delta_{\alpha\beta} \delta_{\beta\gamma}], \end{aligned} \quad (\text{A37})$$

$$\frac{d\sigma}{dt} (qV \rightarrow qV) \Big|_{90^\circ} = \frac{\pi \alpha_s^2}{s^2} [6.11]. \quad (\text{A38})$$

In (A38) the dominant part of the cross section comes from the t -channel gluon-exchange diagram. Naive generalizations of QED when only s - and u -channel quark exchanges are kept can be misleading:

$$\left. \frac{d\sigma}{dt} (VV \rightarrow VV) \right|_{90^\circ} = \frac{\pi\alpha_s^2}{s^2} [31.23] , \quad (\text{A39})$$

$$\left. \frac{d\sigma}{dt} (VV \rightarrow q\bar{q}) \right|_{90^\circ} = \frac{\pi\alpha_s^2}{s^2} [0.15] , \quad (\text{A40})$$

$$\begin{aligned} \left. \frac{d\sigma}{dt} (q\bar{q} \rightarrow VV) \right|_{90^\circ} &= \frac{64}{9} \left. \frac{d\sigma}{dt} (VV \rightarrow q\bar{q}) \right|_{90^\circ} \\ &= \frac{\pi\alpha_s^2}{s^2} [1.04] . \end{aligned} \quad (\text{A41})$$

APPENDIX B: COLOR SUMS

We list here some identities,³³ generalized to $SU(N)$ where appropriate, which are useful in performing the sums over initial and final color states. The summation convention is assumed throughout this discussion.

The qqV vertex involves a factor of T_a ,

$$T_a \equiv \frac{1}{2} \lambda_a , \quad (\text{B1})$$

where the $SU(3)$ matrices, λ_a , are those introduced by Gell-Mann.³⁴ The commutation relations for the T_a are given by the structure constants of the group,

$$[T_a, T_b] = if_{abc} T_c , \quad (\text{B2})$$

$$\{T_a, T_b\} = \frac{4}{N} \delta_{ab} I_{(N)} + 4d_{abc} T_c , \quad (\text{B3})$$

where $I_{(N)}$ is the N -dimensional unit matrix. The f_{abc} are antisymmetric and the d_{abc} are symmetric under the interchange of any two indices. In $SU(2)$, the quantities analogous to (T_a, f_{abc}, d_{abc}) are $(\sigma_i, \epsilon_{ijk}, 0)$. Some useful identities involving the matrices T_a are

$$T_a T_b = \frac{1}{2} \left[\frac{1}{N} \delta_{ab} I_{(N)} + (d_{abc} + if_{abc}) T_c \right] , \quad (\text{B4})$$

$$T_a^{ij} T_a^{kl} = \frac{1}{2} \left(\delta_{il} \delta_{jk} - \frac{1}{N} \delta_{ij} \delta_{kl} \right) , \quad (\text{B5})$$

$$\text{Tr} T_a = 0 , \quad (\text{B6})$$

$$\text{Tr} T_a T_b = \frac{1}{2} \delta_{ab} , \quad (\text{B7})$$

$$\text{Tr} T_a T_b T_c = \frac{1}{4} (d_{abc} + if_{abc}) , \quad (\text{B8})$$

$$\text{Tr} T_a T_b T_a T_c = -\frac{1}{4N} \delta_{bc} . \quad (\text{B9})$$

It is sometimes profitable to define the $(2N-1)$ -dimensional matrices F_a and D_a ,

$$(F_a)_{bc} = -if_{abc} , \quad (\text{B10})$$

$$(D_a)_{bc} = d_{abc} . \quad (\text{B11})$$

The Jacobi identities are

$$f_{abe} f_{ecd} + f_{cbe} f_{aed} + f_{abe} f_{ace} = 0 , \quad (\text{B12})$$

$$f_{abe} d_{ecd} + f_{cbe} d_{aed} + f_{abe} d_{ace} = 0 , \quad (\text{B13})$$

or, equivalently,

$$[F_a, F_b] = if_{abc} F_c , \quad (\text{B12a})$$

$$[F_a, D_b] = if_{abc} D_c . \quad (\text{B13a})$$

A generalization of the $SU(2)$ relation

$$\epsilon_{ijm} \epsilon_{klm} = \delta_{ik} \delta_{jl} - \delta_{il} \delta_{jk} \quad (\text{B14})$$

is

$$\begin{aligned} f_{abc} f_{cde} &= \frac{2}{N} (\delta_{ac} \delta_{bd} - \delta_{ad} \delta_{bc}) \\ &\quad + (d_{ace} d_{bde} - d_{bce} d_{ade}) . \end{aligned} \quad (\text{B15})$$

Some further identities, written in both notations, are

$$f_{abb} = 0 , \quad \text{Tr} F_a = 0 , \quad (\text{B16})$$

$$d_{abb} = 0 , \quad \text{Tr} D_a = 0 , \quad (\text{B17})$$

$$f_{acd} f_{bcd} = N \delta_{ab} , \quad \text{Tr} F_a F_b = N \delta_{ab} , \quad (\text{B18})$$

$$f_{acd} d_{bcd} = 0 , \quad \text{Tr} F_a D_b = 0 , \quad (\text{B19})$$

$$d_{acd} d_{bcd} = \frac{N^2 - 4}{N} \delta_{ab} , \quad \text{Tr} D_a D_b = \frac{N^2 - 4}{N} \delta_{ab} , \quad (\text{B20})$$

$$D_a D_a = \frac{N^2 - 4}{N} I_{(2N-1)} .$$

Specializing to the matrix notation, one has

$$\text{Tr} F_a F_b F_c = i \frac{N}{2} f_{abc} , \quad (\text{B21})$$

$$\text{Tr} D_a F_b F_c = \frac{N}{2} d_{abc} , \quad (\text{B22})$$

$$\text{Tr} D_a D_b F_c = i \frac{N^2 - 4}{2N} f_{abc} , \quad (\text{B23})$$

$$\text{Tr} D_a D_b D_c = \frac{N^2 - 12}{2N} d_{abc} . \quad (\text{B24})$$

The above relations can be used to show

$$\text{Tr} F_a F_b F_a F_c = \frac{N^2}{2} \delta_{bc} . \quad (\text{B25})$$

We now illustrate the use of these relations by calculating some color sums representative of those required in Appendix A.

Consider the $|M_i|^2$ term for $qq \rightarrow qq$. Summing over final color states and averaging over initial states yields

$$\frac{1}{3 \times 3} \text{Tr} T_a T_b \text{Tr} T_a T_b = \frac{1}{9} (\frac{1}{2} \delta_{ab}) = \frac{2}{9} . \quad (\text{B26})$$

The interference term $2M_t M_u^*$ for $qq \rightarrow qq$ has the color sum

$$\frac{1}{3 \times 3} \text{Tr} T_a T_b T_a T_b = -\frac{2}{3} \times \frac{1}{9}. \quad (\text{B27})$$

The interference term $2M_t M_s^*$ for $qV \rightarrow qV$ has color factors

$$\frac{1}{3 \times 8} f_{abc} \text{Tr} T_a T_c T_b = -\frac{i}{4}. \quad (\text{B28})$$

The process $VV \rightarrow VV$ has diagonal terms such as

$$|M_t|^2,$$

$$\begin{aligned} \frac{1}{8 \times 8} f_{aed} f_{ceb} f_{ae'd} f_{ce'b} &= \frac{1}{64} \text{Tr} F_e F_e' \text{Tr} F_e F_e' \\ &= \frac{9}{8}, \end{aligned} \quad (\text{B29})$$

and interference terms such as $2M_t M_u^*$,

$$\begin{aligned} \frac{1}{8 \times 8} f_{aed} f_{ceb} f_{ae'c} f_{de'b} &= \frac{1}{64} \text{Tr} F_a F_b F_a F_b \\ &= \frac{9}{16}. \end{aligned} \quad (\text{B30})$$

*Work performed under the auspices of the United State Energy Research and Development Administration.

¹S. M. Berman, J. D. Bjorken, and J. B. Kogut, Phys. Rev. D **4**, 3388 (1971).

²S. D. Ellis and M. B. Kislinger, Phys. Rev. D **9**, 2027 (1974).

³R. D. Field and R. P. Feynman, Phys. Rev. D **15**, 2590 (1977).

⁴E. Fischbach and G. Look, Phys. Rev. D **15**, 2576 (1977).

⁵R. Hwa, A. J. Speisbach, and M. Teper, Phys. Rev. Lett. **36**, 1418 (1976); Phys. Rev. D (to be published).

⁶R. Cutler and D. Sivers, Phys. Rev. D **16**, 679 (1977).

⁷See, for example, A. De Rújula, H. Georgi, and H. D. Politzer, Ann. Phys. (N.Y.) **103**, 315 (1977).

⁸S. J. Brodsky and G. Farrar, Phys. Rev. Lett. **31**, 1153 (1973); Phys. Rev. D **11**, 1309 (1975).

⁹R. Blankenbecler and S. J. Brodsky, Phys. Rev. D **10**, 2973 (1974).

¹⁰H. Abarbanel, S. Drell, and F. Gilman, Phys. Rev. **177**, 2458 (1969); P. V. Landshoff, J. C. Polkinghorne, and R. Short, Nucl. Phys. **B28**, 225 (1971).

¹¹H. D. Politzer, private communication.

¹²M. Eihorn and S. Ellis, Phys. Rev. D **12**, 2007 (1975).

¹³V. A. Norikov, M. A. Shifman, A. I. Vainshtein, and V. I. Zakharov, Ann. Phys. (N.Y.) **105**, 276 (1977).

¹⁴H. D. Politzer, Phys. Rep. **14C**, 131 (1974).

¹⁵D. Sivers, S. J. Brodsky, and R. Blankenbecler, Phys. Rep. **23C**, 1 (1976).

¹⁶See, for example, V. M. Budnev, I. F. Ginzburg, G. V. Meldon, and V. G. Serfo, Phys. Rep. **15C**, 183 (1975).

¹⁷M. J. Levine, AEC Report No. CAR-882-25, 1971 (unpublished); R. T. Cutler and M. J. Levine, Argonne report, 1976 (unpublished).

¹⁸N. Dombey, J. Phys. **A9**, 1375 (1976); N. Dombey and

C. E. Vayonakis, *ibid.* **A9**, 1381 (1976).

¹⁹V. Elias, J. C. Pati, A. Salam, and J. Strathdee, Pramana **8**, 303 (1977).

²⁰B. Alper *et al.*, Nucl. Phys. **B100**, 237 (1975).

²¹F. W. Büsser *et al.*, Nucl. Phys. **B106**, 1 (1976).

²²R. Blankenbecler, S. J. Brodsky, and J. F. Gunion, Phys. Lett. **39B**, 649 (1972); Phys. Rev. D **6**, 2652 (1972); Phys. Lett. **42B**, 461 (1973).

²³See, for example, T. K. Gaisser, Report No. BNL-21650, Proceedings of the VII International Colloquium on Multiparticle Reactions, Tutzing, Germany, 1976 (unpublished).

²⁴P. Darriulat *et al.*, Nucl. Phys. **B107**, 429 (1976) (CERN R412 Experiment); M. Della Negra *et al.*, Report No. CERN/EP/Phys. 76-43 (CCHK collaboration) (unpublished).

²⁵R. P. Feynman, R. D. Field, and G. C. Fox, Report No. CALT-68-595 (unpublished).

²⁶H. D. Politzer, Report No. HUTP-77/A029, 1977 (unpublished).

²⁷P. Stix, C. Bromberg, T. Ferbel, T. Jensen, and P. Slattery, Phys. Rev. D **16**, 558 (1977).

²⁸D. H. Perkins, P. Schreiner, and W. G. Scott, Phys. Lett. **67B**, 347 (1977).

²⁹C. Bromberg *et al.*, Phys. Rev. Lett. **38**, 1447 (1977).

³⁰See, for example, S. D. Ellis, Phys. Lett. **49B**, 189 (1974). G. Preparata, Nucl. Phys. **B80**, 299 (1974).

³¹D. W. Duke, Phys. Rev. D **16**, 1375 (1977). Statements in this paper about the importance of gluon scattering do not refer to QCD, but to a model in which gluons do not self-couple.

³²B. L. Combridge, J. Kripfganz, and J. Ranft, Phys. Lett. **70B**, 234 (1977).

³³A. J. Macfarlane, A. Sudbery, and P. H. Weisz, Commun. Math. Phys. **11**, 77 (1968).

³⁴M. Gell-Mann, Phys. Rev. **125**, 1067 (1962).